OXFORD

Cerebral Cortex, March 2020;30: 1752–1767

doi: 10.1093/cercor/bhz200
Advance Access Publication Date: 11 October 2019
Original Article

ORIGINAL ARTICLE

Quantitative In vivo MRI Assessment of Structural Asymmetries and Sexual Dimorphism of Transient Fetal Compartments in the Human Brain

Lana Vasung[1,2,*], Caitlin K. Rollins[3,4], Hyuk Jin Yun[1,2], Clemente Velasco-Annis[3], Jennings Zhang[1,5], Konrad Wagstyl[6], Alan Evans[5], Simon K. Warfield[3], Henry A. Feldman[2,7], P. Ellen Grant[1,2,*] and Ali Gholipour[3,*]

[1]Fetal-Neonatal Neuroimaging & Developmental Science Center (FNNDSC), Boston, MA 02115, USA [2]Division of Newborn Medicine, Boston Children's Hospital, Harvard Medical School, Boston, MA 02115, USA [3]Computational Radiology Laboratory, Boston Children's Hospital, Harvard Medical School, Boston, MA 02115, USA [4]Department of Neurology, Boston Children's Hospital, Harvard Medical School, Boston, MA 02115, USA [5]McGill Centre for Integrative Neuroscience/Montreal Neurological Institute, McGill University, Montreal QC H3A 2B4, Canada [6]University of Cambridge, Cambridge CB2 8AH, UK [7]Institutional Centers for Clinical and Translational Research, Boston Children's Hospital, Harvard Medical School, Boston, MA 02115, USA

Address correspondence to Lana Vasung, Division of Newborn Medicine, Boston Children's Hospital, Harvard Medical School, Boston, MA 02215, USA. Email: lana.vasung@childrens.harvard.edu
*Lana Vasung, P. Ellen Grant and Ali Gholipour are co-authors co-authors.

Abstract

Structural asymmetries and sexual dimorphism of the human cerebral cortex have been identified in newborns, infants, children, adolescents, and adults. Some of these findings were linked with cognitive and neuropsychiatric disorders, which have roots in altered prenatal brain development. However, little is known about structural asymmetries or sexual dimorphism of transient fetal compartments that arise in utero. Thus, we aimed to identify structural asymmetries and sexual dimorphism in the volume of transient fetal compartments (cortical plate [CP] and subplate [SP]) across 22 regions. For this purpose, we used in vivo structural T2-weighted MRIs of 42 healthy fetuses (16.43–36.86 gestational weeks old, 15 females). We found significant leftward asymmetry in the volume of the CP and SP in the inferior frontal gyrus. The orbitofrontal cortex showed significant rightward asymmetry in the volume of CP merged with SP. Males had significantly larger volumes in regions belonging to limbic, occipital, and frontal lobes, which were driven by a significantly larger SP. Lastly, we did not observe sexual dimorphism in the growth trajectories of the CP or SP. In conclusion, these results support the hypothesis that structural asymmetries and sexual dimorphism in relative volumes of cortical regions are present during prenatal brain development.

Key words: cortical plate, fetus, in vivo MRI, subplate, transient fetal compartments

Introduction

The research into structural asymmetry of the human brain began with an early work of Leuret and Gratiolet (1839), who showed that an asymmetric pattern of cortical convolutions is present in humans. Origins of research into functional lateralization of the human brain date to early work of Pierre Paul Broca. Based on the lesion studies, Broca (1865) proposed a novel concept of functional brain lateralization according to which the left hemisphere is entirely responsible for speech. Thus, the majority of researchers at that time thought that structural asymmetry and functional lateralization of the brain are human-specific. Nevertheless, almost a century later, many studies confirmed the existence of structural asymmetries and functional lateralization in species other than humans (Rogers and Anson 1979; Matsuo et al. 2010; Frasnelli 2013; Smaers 2013; Heuer et al. 2018). Even though today we are able to identify structural brain asymmetries (Kong et al. 2018) and characterize lateralization of specific brain functions across a large number of human subjects (Karolis et al. 2019), the time at which these structural asymmetries arise remain unknown.

Language and handedness in humans are two brain functions that are remarkably lateralized and thought to be genetically determined through structural brain asymmetries. The heritability of cortical asymmetries, estimated by measuring the regional cortical thickness and surface area, has been recently identified in a large number of subjects (Kong et al. 2018). In contrast, the role of heritability in functional lateralization remains difficult to apprehend (Medland et al. 2009). Single-nucleotide polymorphisms (SNPs) of the *PCSK6* gene, which regulate the left–right body axis formation, have been linked to handedness (Scerri et al. 2011; Brandler et al. 2013; Robinson et al. 2016). Similarly, SNPs of the *FOXP2* gene, which code transcription relevant for the structural development of the language-related brain regions, were associated with the language lateralization (Ocklenburg et al. 2013). In addition to genetic variation, epigenetic regulation of the genes also appears to play an important role. For example, the level of methylation of certain genes was reported to be associated with the strength of lateralization of particular brain functions, such as handedness (Leach et al. 2014). Still, effect sizes produced by variations in genes within a single locus remain very small. Therefore, the genetic basis for structural asymmetry and functional brain lateralization is most likely determined by polygenes, some of which are transiently expressed during prenatal brain development (Kang et al. 2011; Li et al. 2018). To identify origins of hemispheric structural asymmetries, the best approach would be to characterize hemispheric asymmetries in cortical regions of the adult brain and to evaluate the development of these regions throughout prenatal development.

In the adult human brain, leftward asymmetries were found in cortical regions and fiber tracts relevant for language, such as inferior frontal and superior temporal gyrus and arcuate fascicle (Büchel et al. 2004; Kong et al. 2018). Handedness-related structural asymmetries have been reported but predominantly in the white matter regions underlying the precentral gyrus (Büchel et al. 2004). In addition, there are significant effects of the sex on structural brain asymmetry. For example, adult males compared to females tend to have more pronounced rightward asymmetry of the cortical surface (Kong et al. 2018). However, larger effects of sex were found in cortical surface and thickness asymmetry in younger females (Kong et al. 2018). Structural brain asymmetries have been reported even in prematurely born infants (Dubois et al. 2008). However, it remains unresolved whether these structural asymmetries arise in utero, whether they are under strong influences of prenatal testosterone (Geschwind and Galaburda 1985), or whether they are shaped principally by our postnatal experiences.

Postmortem studies of the human fetal brain have been mostly focused on characterizing the morphology of the cortical landscape and measuring the cranial fossae (Eberstaller 1890; Cunningham 1892; Retzius 1896; Hrdlička 1907; Chi et al. 1977a). Advances in in vivo fetal MRI acquisition and MRI postprocessing techniques now allow reliable reconstruction of in utero fetal brains in 3D space. Consequently, many findings of in vivo MRI studies confirmed already known observations from "postmortem autopsies." Thus, it has been generally accepted that during mid-gestation, gyri and sulci of the right hemisphere in the perisylvian region appear earlier compared to the ones on the left (Kasprian et al. 2011; Habas et al. 2012).

The studies of hemispheric differences and sex effects on the regional growth of transient fetal compartments in the human brain are scarce. In the light of the aforementioned findings, along with the lack of dedicated quantitative studies of transient fetal compartments, the mechanism leading to the appearance of cortical asymmetries remains unexplained. In other words, it remains unclear whether the asymmetries of the cortical convolutions in the fetal brain are a result of different tangential and radial growth between cortical and subcortical transient compartments. Despite the reported asymmetries in cortical curvature, gene expression studies failed to show asymmetries in gene expression between neocortical regions during prenatal fetal brain development (Hawrylycz et al. 2012; Pletikos et al. 2014), suggesting a large effect of intrauterine and extrauterine environment on brain lateralization.

In this study, we have used in vivo fetal brain MRIs to characterize structural asymmetries across 22 fetal cortical regions. During prenatal development, the fetal brain is composed of transient fetal compartments (Bystron et al. 2006). The most superficial fetal transient compartments are the marginal zone (a thin layer of neurons situated beneath the pia), the cortical plate (CP, a layer-like compartment composed of densely packed postmigratory neurons that is situated beneath the marginal zone and is often called the "future cortex") and the subplate (SP, a transient fetal compartment situated just beneath the CP). Given that the CP and SP are composed of neurons with the first functional axodendritic synapses (Molliver et al. 1973), for the purpose of this study CP and SP of a particular region were grouped together and were called the "fetal cortex." In order to identify which sub-component of the fetal cortex displays structural differences related to growth, hemisphere, and sex, we also measured volumes of the SP and CP within the 22 parcellated cortical regions.

Materials and Methods

Materials

In vivo MRIs of 42 healthy fetuses (16.43–36.86 gestational weeks (GW), 15 females) were acquired on a 3T Siemens Skyra MRI scanner using multiple T2-weighted (T2w) Half-Fourier Single Shot Turbo Spin Echo scans with following parameters: TR = 1400–2000 ms, TE = 100–120 ms, in-plane resolution 0.9–1.1 mm, and a 2-mm slice thickness (for details of MR image acquisition, see (Gholipour et al. 2017)).

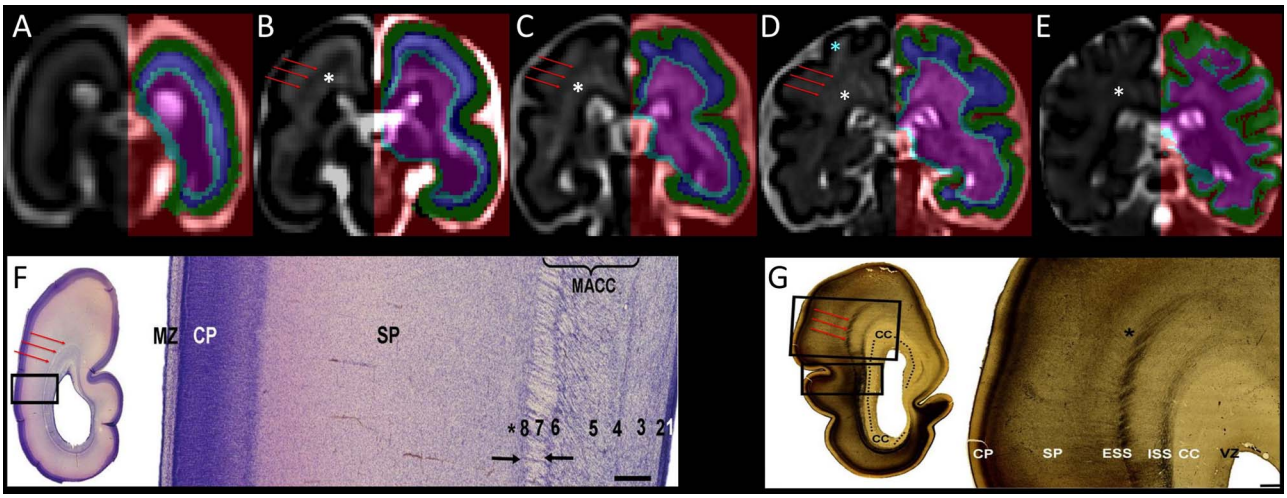

Figure 1. Coronal sections showing the segmentation of the telencephalic wall into transient fetal compartments (CP in green, SP in blue, and IZ with subcortical structures in light blue and pink) in 21.57 (A), 24.71 (B), 27.71 (C), 31.57 (D), and 34.14 (E) GW fetal brains. Transient fetal compartments were identified by using anatomical landmarks and the histological descriptions from Nissl (F) and AChE (G) stained sections (F and G were reproduced with permission from (Žunić Išasegi et al. 2018)). The superficial external sagittal stratum (red arrows) was used as a continuous border between the SP and the IZ. Note that the MR signal intensity varies within the SP (T2w hyperintense regions of the superficial SP within the gyral crowns are shown with blue asterisk) and the intermediate zone (periventricular crossroads are marked with the white asterisks (Judaš et al. 2005; Kidokoro et al. 2011; Girard et al. 2012). MACC, multilaminar axonal-cellular compartment; ISS, internal sagittal stratum; CC, corpus callosum; MZ, marginal zone; VZ, ventricular zone. VZ (1), inner subventricular zone (2), periventricular (callosal) fiber-rich zone (3), complex fibrillar/cellular stratum composed of the outer subventricular zone (OSVZ) and an inner (proliferative) cell layer (4–6), external sagittal stratum with strictly packed thalamocortical projection fibers (7), and external transient (proliferative) cell band (8) (descriptions reproduced with permission from (Žunić Išasegi et al. 2018)). Associative fibers along the border between the deep SP and the superficial IZ are marked with the black asterisks.

Methods

Identification of Transient Fetal Compartments

MRIs were first preprocessed with an in-house built pipeline, as previously described (Gholipour et al. 2017). This pipeline composed of the following steps: 1) motion correction and 3D reconstruction with isotropic super-resolution (Kainz et al. 2015), 2) brain masking (Mohseni Salehi et al. 2017), 3) N4 bias field correction with intensity normalization (Tustison et al. 2010), and 4) rigid registration to a spatiotemporal fetal brain MRI atlas (Gholipour et al. 2017).

Next, two independent readers with expertise in fetal anatomy (PEG and LV) reviewed the MRIs and identified the transient fetal compartments according to the histological (Kostovic and Rakic 1990; Kostović et al. 2002; Bakken et al. 2016; Molnár and Hoerder-Suabedissen 2016; Vasung et al. 2016; Krsnik et al. 2017; Kostović et al. 2018a; Žunić Išasegi et al. 2018) and MRI (Kostović et al. 2002, 2014; Perkins et al. 2008; Huang et al. 2009; Vasung et al. 2016, 2017; Diogo et al. 2018) descriptions.

Fetal structures and transient fetal compartments, which are radially arranged across the telencephalic wall, were identified based on their T2w signal intensities as follows (Figs S1–3):

1) Subarachnoid space with cerebrospinal fluid, which is characterized by a high T2w MR signal intensity (Figs S1–3, voxels in red color).
2) Cortical plate (CP) of low T2w MR signal intensity (Figs S1–3, voxels in green color).
3) Subplate (SP) of high-to-moderate T2w MR signal intensity (Figs S1–3, voxels in blue color).
4) Intermediate zone (IZ) of moderate T2w MR signal intensity (Figs S1–3, voxels in pink color).
5) Proliferative compartments (i.e., ventricular zone, subventricular zone SVZ, and ganglionic eminence), which are lining the walls of the lateral ventricles, of low T2w MR signal intensity (Figs S1–3, voxels in yellow color).

Transient fetal compartments were automatically segmented as previously described (Gholipour et al. 2017). In the next step, the segmentations were manually refined (Fig. 1A–E) using the MNI Display software (http://www.bic.mni.mcgill.ca/software/Display/Display.html).

Given that the T2w MR signal intensity is not homogenous within transient fetal compartments (Figs S1–3), in particular within the SP and IZ, anatomical guidelines derived from the histological studies (Vasung et al. 2010; Kostović et al. 2018a; Žunić Išasegi et al. 2018) were used to identify the borders between transient compartments. In particular, the superficial external sagittal stratum (ESS), which corresponds to the primordial external capsule (Fig. 1F,G; Žunić Išasegi et al. 2018), was identified as a hypointense band on T2w MR images (red arrows in Fig. 1). The ESS was used as a continuous border between SP and IZ (Fig. 1A–E).

Surfaces of the transient fetal compartments (CP, SP, and IZ, Fig. 2A,D,G) were extracted using the modified CIVET pipeline described previously (Vasung et al. 2016).

On the reconstructed pial surfaces (Fig. 2A,D,G, in green) and SP (Fig. 2A,D,G, in cyan), we have manually painted 24 regions of interest (ROIs) according to the Desikan–Killiany atlas (Desikan et al. 2006)(Fig. 3) taking into account the appearance (Chi et al. 1977a; Garel et al. 2001; Girard and Gambarelli 2001; Fogliarini et al. 2005; Dubois et al. 2008; Habas et al. 2012; Yun et al. 2018) and the variations of the sulcal roots and fissures (Eberstaller 1890; Smith 1904a, 1904b; von Economo and Koskinas 1925; Ono et al. 1990; Germann et al. 2005; Iaria and Petrides 2007; Zlatkina and Petrides 2010; Duvernoy 2012; Segal and Petrides 2012) (Fig. 2B,E,H). In younger brains, with very few sulcal landmarks, cortical ROIs were derived from 1 week older brains

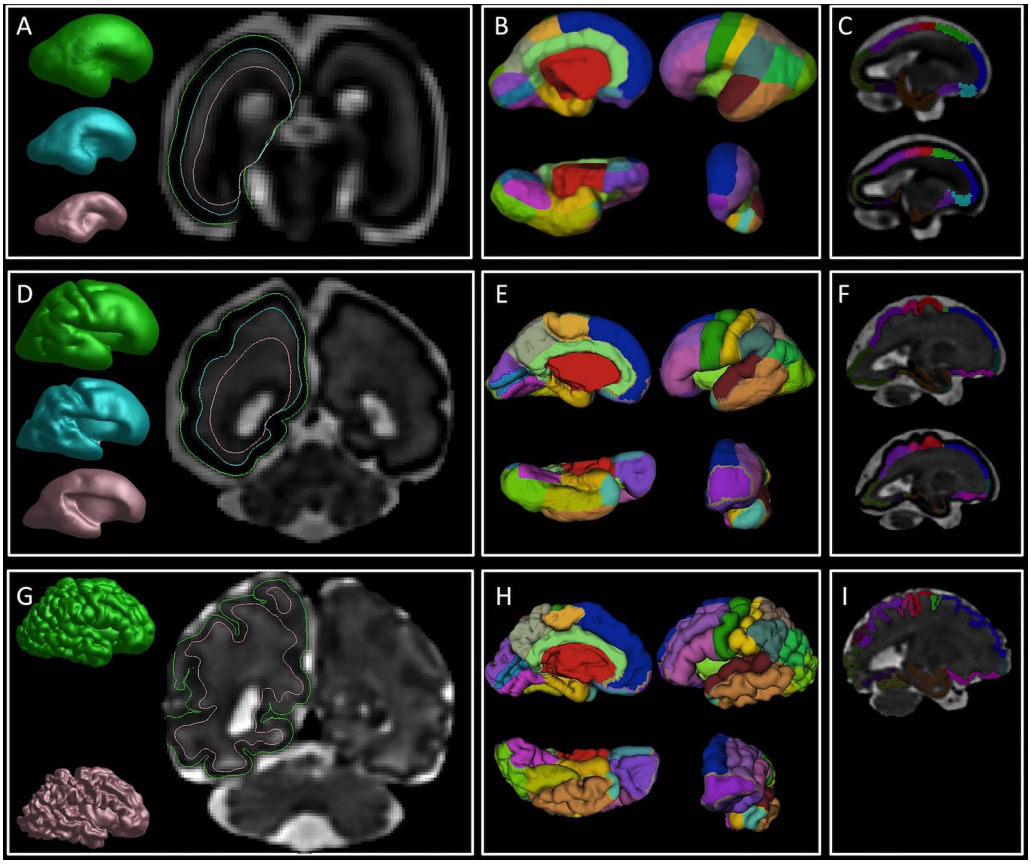

Figure 2. An overview of the image processing steps. First column: reconstruction of the pial (green), SP (cyan), and IZ (pink) surfaces in 25 (*A*), 29.57 (*D*), and 36.86 (*G*) GW brain. Note the borders of the reconstructed surfaces that are superimposed on the coronal sections and mark the border between fetal compartments. Second column: manually painted cortical ROIs superimposed on the reconstructed pial surface in 25 (*B*), 29.57 (*E*), and 36.86 (*H*) GW brain. Third column: volumetric ROIs of CP (upper row in *C*, *F*, and *I*) and SP (bottom row in *C* and *F*) in 25 (*C*), 29.57 (*F*), and 36.86 (*I*) GW brain.

by coregistering the surfaces and manually refining the ROIs (Fig. 2*B*,*E*,*H*).

Due to the high variability and branching of rhinal, collateral, occipitotemporal, and inferior temporal sulci, regions of fusiform, middle, and inferior temporal gyri were grouped together with the temporal pole into one region called latero-inferior temporal neocortex. Thus, our parcellation resulted in 22 fetal cortical regions that were included in the final analysis.

Finally, the labels of painted surface ROIs were projected to the underlying CP or SP voxels using the in-house built software (Fig. 2*C*,*F*,*I*). The volumetric ROIs of the CP or SP were coregistered with the initially segmented CP masks using the ANTS non-linear coregistration tool (Avants et al. 2011).

Measurement of Regional Volumes of the Fetal Cortex and Transient Fetal Compartments

Regional volumes of the fetal cortex (comprising a CP and SP) were calculated in mm^3 using the ITK-snap software. Regional volumes of transient fetal compartments in mm^3 (CP or SP) were also calculated separately using the ITK-snap software.

Statistical Analysis

All of the regional volumes showed skewed distributions and were log-transformed for statistical analysis. For each of the 22 regions, we constructed a mixed-effects linear model with log-transformed volume as the dependent variable and the following factors as independent variables: hemisphere (left or right), transient fetal compartment (CP or SP), sex, and gestational age (GA) of the fetus. We included interaction terms to allow the effect of GA (i.e., growth rate) to vary by sex, hemisphere, and transient fetal compartment. We included additional terms to allow potential interactions of sex × hemisphere, sex × compartment, and compartment × hemisphere, and a subject-specific Gaussian offset (random effect) to account for correlation among the multiple measurements from a given fetus. We fitted the model using SAS software (version 9.4, Cary, NC) and confirmed a quasi-Gaussian distribution of residuals. From the parameters of the fitted model, we constructed estimates for 13 comparisons of interest (Table 1–6, Table S1, Table S2), including growth rates and left–right differences, with standard errors derived from the pooled variance. We tested each comparison for significant deviation from zero by dividing the estimate by its standard error and referring the ratio to the *t*-distribution. We applied the Holm step-down procedure to adjust the *P* values for multiple comparisons and enforce a maximum experiment-wise Type I error rate of 5% over the 13 tests conducted for each region. For reporting, we converted each contrast, Δlog volume, to a percentage ($\%\Delta = 100\% \times (\exp(\Delta\text{log volume})—1)$, with standard error SE ($\%\Delta$) = $\Delta\% \times (\exp(\text{SE}(\Delta\text{log volume}))—1)$ and 95% confidence limits Limit ($\%\Delta$) = $100\% \times (\exp(\text{Limit}(\Delta\text{log volume}))—1)$.

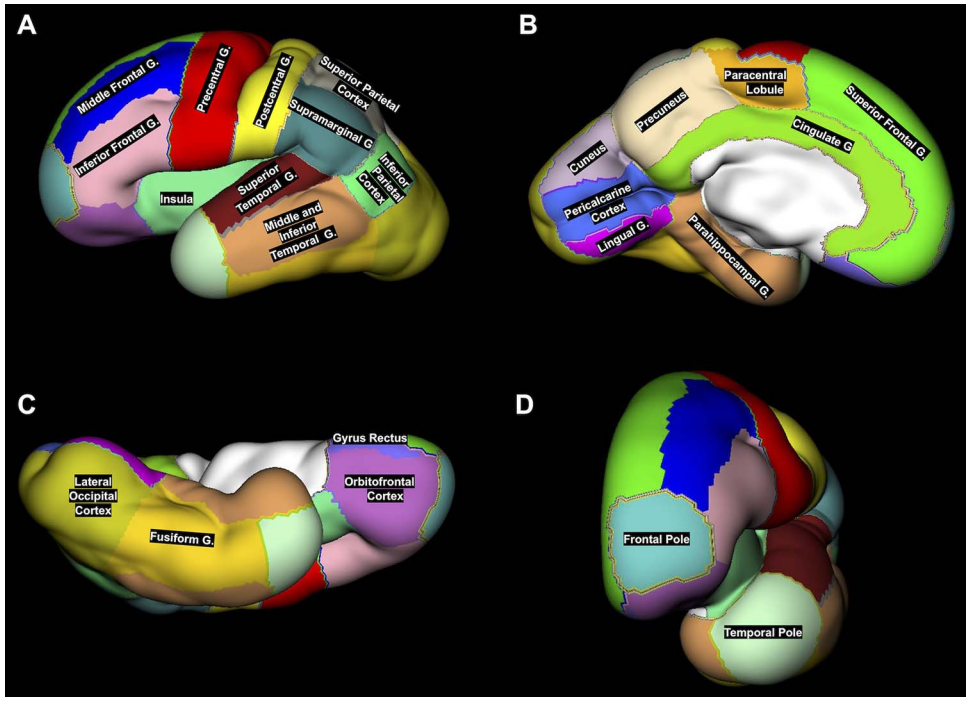

Figure 3. An example of 24 ROIs manually segmented on the reconstructed CP surface (lateral (A), medial (B), ventral (C), and anterior (D) views) of the left hemisphere in 29.57 GW fetus. Note that the middle and inferior temporal gyri were merged with temporal pole and fusiform gyrus into one region called latero-inferior temporal neocortex.

Results

Age-Related Changes of the Fetal Cortex (Comprising CP and SP)

Age-related volume growth of the fetal cortex (comprising a CP and SP) was statistically significant for each region of the left and right hemisphere. The average relative volume growth of the fetal cortex per each gestational week, together with the confidence intervals, can be found in the Table 1 and Fig. 4.

Among the 22 fetal cortical regions, the relative growth of the fetal cortex had the fastest growth rate in the occipital lobes (lingual gyrus bilaterally, left pericalcarine cortex and left cuneus) and regions of the right inferior parietal lobule. However, the relative volume increase of transient fetal zones (CP and SP) varied among cortical regions.

In regions of the superior temporal cortex, the relative growth of the CP was significantly faster compared to the growth of the SP (mean ± SD = 4.8 ± 0.8, CI = [3.1, 6.5], $P < 0.001$, adjusted). In contrast, the growth of the CP was significantly slower compared to the SP in cortical regions of the lingual gyrus (mean ± SD = −9.7 ± 1.9, CI = [−13.4, −5.9], $P = 0.001$, adjusted), cuneus (mean ± SD = −9.6 ± 1.8, CI = [−13.1, −5.9], $P < 0.001$, adjusted), and latero-inferior occipital cortex (mean ± SD = −5.3 ± 1, CI = [−7.3, −3.3], $P < 0.001$, adjusted) (Fig. S4, Table S1).

Regional Differences in the Volume of the CP and SP

We tested if there were significant differences in the volume of the SP, compared to the CP, in the given region.

During prenatal development, the relative volume of the CP was significantly larger compared to the volume of the underlying SP in numerous frontal, temporal, occipital, and limbic regions (adjusted (Table 2, Fig. S5)). In contrast, we did not observe significant differences in the relative volume between the CP and SP in majority of central and parietal regions (Table 2, Fig. S5).

Sex differences

Females had significantly smaller relative volumes of the left inferior frontal gyrus (mean ± SD = −32.2 ± 7.2, CI = [−44.5, −17.2], $P = 0.046$, adjusted), whilst no significant differences of the right hemisphere were found between sexes (Table 3).

We did not find significant differences in the relative volume of the CP between females and males (adjusted for hemisphere and age). However, compared to the males, females had a significantly smaller relative volume of the SP in the inferior frontal gyrus (mean ± SD = −34.1 ± 7.5, CI = [−46.8, −18.3], $P = 0.004$, adjusted), cingulate gyrus (mean ± SD = −48.1 ± 8.2, CI = [−61.2, −30.6], $P = 0.005$, adjusted), and calcarine cortex (mean ± SD = −52.3 ± 8.8, CI = [−66, −33.1], $P = 0.009$, adjusted) (Table 4, Fig. 5).

Finally, no significant difference was found in the growth of cortical regions between males and females (Table S2).

Hemispheric Differences

First, we tested if there were significant differences in the volume of the fetal cortex (composed of SP and CP) in the given region during entire prenatal development.

We found a significant leftward asymmetry of the inferior frontal gyrus and rightward asymmetry of the orbitofrontal fetal cortex, adjusted for the effects of age and sex (Table 5).

Table 1 Increase in the relative volume of the cortical region (combined volume of the CP and SP) per gestational week

	Left hemisphere			Right hemisphere		
	Increase (%) ± standard error	[Confidence intervals]	Adjusted *P* value	Increase (%) ± standard error	[Confidence intervals]	Adjusted *P* value
Inferior frontal gyrus	12.3 ± 1.1	[10.1, 14.5]	<**0.001** *	15.6 ± 1.2	[13.3, 17.9]	<**0.001** *
Orbitofrontal cortex	19.6 ± 1.7	[16.2, 23.1]	<**0.001** *	19.6 ± 1.8	[16.2, 23.1]	<**0.001** *
Frontal pole	16.4 ± 2.1	[12.4, 20.6]	<**0.001** *	17.6 ± 2.0	[13.8, 21.5]	<**0.001** *
Lingual gyrus	22.2 ± 2.1	[18.1, 26.4]	<**0.001** *	29.6 ± 2.2	[25.3, 34.1]	<**0.001** *
Precuneus	16.3 ± 1.1	[14.0, 18.6]	<**0.001** *	15.1 ± 1.1	[12.9, 17.3]	<**0.001** *
Occipital cortex	10.9 ± 1.2	[8.5, 13.3]	<**0.001** *	13.3 ± 1.2	[10.9, 15.7]	<**0.001** *
Precentral gyrus	16.3 ± 1.0	[14.4, 18.3]	<**0.001** *	17.3 ± 1.1	[15.2, 19.4]	<**0.001** *
Superior temporal gyrus	12.0 ± 1.0	[10.0, 14.0]	<**0.001** *	12.9 ± 1.0	[11.0, 14.9]	<**0.001** *
Middle frontal gyrus	15.1 ± 1.1	[13.0, 17.2]	<**0.001** *	16.1 ± 1.1	[14.0, 18.2]	<**0.001** *
Calcarine cortex	20.7 ± 2.0	[16.8, 24.7]	<**0.001** *	19.1 ± 2.0	[15.3, 23.1]	<**0.001** *
Insula	11.5 ± 1.5	[8.6, 14.6]	<**0.001** *	11.3 ± 1.5	[8.4, 14.3]	<**0.001** *
Superior frontal gyrus	11.8 ± 0.8	[10.3, 13.3]	<**0.001** *	13.1 ± 0.8	[11.5, 14.6]	<**0.001** *
Supramarginal gyrus	16.5 ± 1.1	[14.2, 18.8]	<**0.001** *	14.3 ± 1.1	[12.1, 16.6]	<**0.001** *
Postcentral gyrus	15.5 ± 1.0	[13.4, 17.5]	<**0.001** *	16.4 ± 1.0	[14.4, 18.5]	<**0.001** *
Parahippocampal gyrus	18.3 ± 2.6	[13.2, 23.5]	<**0.001** *	15.0 ± 2.5	[10.2, 20.1]	<**0.001** *
Superior parietal lobule	10.8 ± 0.9	[9.0, 12.7]	<**0.001** *	11.0 ± 0.9	[9.2, 12.8]	<**0.001** *
Cuneus	27.2 ± 1.9	[23.5, 31.0]	<**0.001** *	15.7 ± 1.8	[12.2, 19.3]	<**0.001** *
Paracentral lobule	15.3 ± 1.1	[13.1, 17.5]	<**0.001** *	14.7 ± 1.1	[12.6, 16.9]	<**0.001** *
Inferior parietal lobule	17.4 ± 1.0	[15.3, 19.4]	<**0.001** *	21.9 ± 1.1	[19.7, 24.1]	<**0.001** *
Gyrus rectus	21.9 ± 3.0	[16.1, 28.0]	<**0.001** *	20.7 ± 3.2	[14.6, 27.1]	<**0.001** *
Latero-inferior temporal neocortex	17.8 ± 1.1	[15.7, 20.0]	<**0.001** *	17.2 ± 1.0	[15.1, 19.3]	<**0.001** *
Cingulate gyrus	16.6 ± 1.6	[13.5, 19.9]	<**0.001** *	18.0 ± 1.6	[14.8, 21.2]	<**0.001** *

*Significant correlations after correction for multiple comparisons.

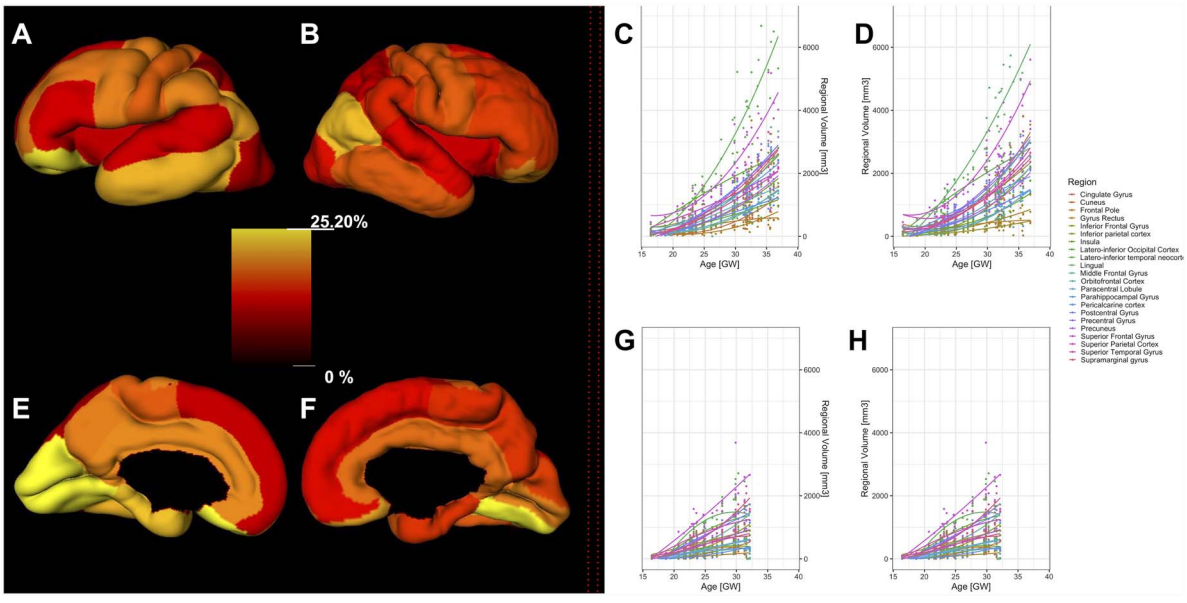

Figure 4. Relative regional volume growth (*A*, *B*, *E*, *F*) of the fetal cortex (comprising CP and SP) and absolute regional growth of the CP (*C*, *D*) and SP (*G*, *H*) during prenatal development. All regions showed significant age-related changes in the relative volume of the fetal cortex. Left columns (*A*, *B*, *E*, *F*): the relative percentages of the regional volume increase of the fetal cortex are superimposed on a reconstructed pial surface of the left (*A*, *E*) and right hemisphere (*B*, *F*) in the 27.71 GW fetus. The color-coded bar in the center indicates a relative increase in the volume per week of gestation. Right columns (*C*, *D*, *G*, *H*): scatter plots of absolute volumes (y-axes) of the fetal compartments at a given age (GW, x-axes). CP volumes (left (*C*) and right hemisphere (*D*)) and SP volumes (left (*G*) and right hemisphere (*H*)) are shown together with the second degree polynomial curves.

Table 2 Differences in the relative mean volumes between the CP and SP in the left and right hemisphere across prenatal development

	Left hemisphere			Right hemisphere		
	Increase (%) ± standard error	[Confidence intervals]	Adjusted *P* value	Increase (%) ± standard error	[Confidence intervals]	Adjusted *P* value
Inferior frontal gyrus	49.0 ± 9.8	[31.3, 69.1]	<**0.001***	57.4 ± 10.3	[38.7, 78.6]	<**0.001***
Orbitofrontal cortex	80.0 ± 21.2	[44.2, 124.6]	<**0.001***	67.4 ± 20.0	[33.7, 109.5]	**0.004***
Frontal pole	11.6 ± 14.0	[−11.8, 41.3]	>1	73.6 ± 21.2	[38.0, 118.4]	**0.002***
Lingual gyrus	84.9 ± 23.2	[46.1, 134.1]	<**0.001***	87.5 ± 23.0	[48.9, 136.1]	<**0.001***
Precuneus	17.5 ± 8.2	[2.7, 34.5]	>1	18.7 ± 8.3	[3.8, 35.8]	>1
Occipital cortex	80.3 ± 11.4	[59.6, 103.6]	<**0.001***	53.3 ± 9.6	[35.8, 73.1]	<**0.001***
Precentral gyrus	6.2 ± 5.5	[−4.0, 17.5]	>1	1.7 ± 5.3	[−8.0, 12.5]	>1
Superior temporal gyrus	48.3 ± 6.9	[35.4, 62.5]	<**0.001***	47.7 ± 6.9	[34.9, 61.7]	<**0.001***
Middle frontal gyrus	28.7 ± 7.8	[14.5, 44.6]	**0.010***	34.0 ± 8.1	[19.3, 50.6]	<**0.001***
Calcarine cortex	275.5 ± 43.3	[202.0, 366.8]	<**0.001***	273.4 ± 43.2	[200.3, 364.4]	<**0.001***
Insula	57.1 ± 16.3	[29.1, 91.2]	<**0.001***	74.9 ± 17.4	[44.8, 111.2]	<**0.001***
Superior frontal gyrus	2.4 ± 4.5	[−6.0, 11.5]	>1	−0.9 ± 4.3	[−9.0, 7.8]	>1
Supramarginal gyrus	−0.5 ± 6.0	[−11.4, 11.7]	>1	3.8 ± 6.2	[−7.5, 16.6]	>1
Postcentral gyrus	8.9 ± 6.5	[−2.9, 22.1]	>1	3.0 ± 6.1	[−8.1, 15.6]	>1
Parahippocampal gyrus	424.6 ± 100.9	[269.6, 644.7]	<**0.001***	469.2 ± 105.9	[305.2, 699.5]	<**0.001***
Superior parietal lobule	11.3 ± 6.7	[−1.0, 25.0]	>1	11.6 ± 6.7	[−0.6, 25.4]	>1
Cuneus	39.5 ± 18.4	[9.0, 78.6]	>1	44.1 ± 18.9	[12.9, 84.1]	>1
Paracentral lobule	14.6 ± 8.6	[−0.7, 32.3]	>1	12.6 ± 8.4	[−2.4, 29.9]	>1
Inferior parietal lobule	18.3 ± 8.5	[3.0, 35.7]	>1	9.0 ± 7.8	[−5.0, 25.1]	>1
Gyrus rectus	150.2 ± 57.7	[65.5, 278.3]	<**0.001***	74.3 ± 40.4	[15.2, 163.9]	>1
Latero-inferior temporal neocortex	60.0 ± 9.4	[42.8, 79.2]	<**0.001***	66.2 ± 9.7	[48.4, 86.2]	<**0.001***
Cingulate gyrus	83.1 ± 19.9	[49.1, 124.8]	<**0.001***	123.2 ± 25.3	[80.2, 176.5]	<**0.001***

*Significant correlations after correction for multiple comparisons.

Inferior frontal gyrus of the left hemisphere, composed of SP and CP, was on average 25.6% larger (SD = 5.3, CI = [15.5, 36.3], *P* = 0.001) compared to the inferior frontal gyrus of the right hemisphere (Fig. 6, Table 5). In contrast, the orbitofrontal cortex, composed of SP and CP, was on average 26.8% larger in the right hemisphere (SD = 5.6, CI = [15.2, 36.7], *P* = 0.013).

Next, we tested if there were significant differences in the volume of the SP or CP in the given region during the entire prenatal development. As expected, we also found structural asymmetry in the volume of the SP and CP in frontal regions (Table 6). The CP of the inferior frontal gyrus was on average 22.2% larger in the left hemisphere (SD = 6.5, CI = [10.2, 35.4], *P* = 0.04). Similarly, the SP volume of the inferior frontal gyrus was on average 29% larger in the left hemisphere (SD = 8.6, CI = [13.5, 46.5], *P* = 0.03). The SP of the frontal pole was also found to be significantly larger in the left hemisphere (CI = [31, 112.3], *P* = 0.014).

Discussion

To our knowledge, this is the first study to address structural asymmetries and sexual dimorphism in the volumes of fetal cortex (composed of CP and SP) and in the volumes of transient fetal compartments (CP or SP) across 22 cortical regions during prenatal brain development. As expected, the relative volume of the fetal cortex (defined as the CP and SP) significantly increased with age. In the majority of regions, with the exception of central regions, the relative volume of the CP was significantly larger compared to the SP (adjusted). Throughout the prenatal development, there was no significant difference in relative age-related volume growth of SP and CP, except in regions of superior temporal gyrus (faster growth of CP) and occipital lobes (more rapid growth of SP in latero-inferior occipital cortex, cuneus and lingual gyrus).

Furthermore, males, compared to females, had significantly larger relative volumes of regions belonging to limbic lobe (cingulate gyrus), occipital lobe (pericalcarine cortex), and frontal lobe (inferior frontal gyrus). In these regions, the sexual dimorphism in volume was driven by the larger volumes of the SP compartment.

In addition to the sexual dimorphism, we also found hemispheric asymmetries in volumes. A significant leftward asymmetry in the volume of the CP and the volume of the SP was found in inferior frontal gyrus, while significant rightward asymmetry in the volume of fetal cortex was found in the orbitofrontal region.

Together, these results indicate that the relative growth in the volume of SP and the CP is synchronous across the majority of regions and does not show sexual dimorphism in growth trajectories. However, hemispheric asymmetries and sexual dimorphism in relative volumes of transient fetal compartments do exist, in particular in regions related to language function (inferior frontal gyrus). These differences could reflect cytoarchitectonic differences in the cellular composition of these regions between males and females as well as between hemispheres during prenatal fetal development.

Table 3 Differences between females and males in the relative regional volumes of the cortex (CP combined with SP) per hemisphere

	Left hemisphere			Right hemisphere		
	Difference (%) ± standard error	(Confidence intervals)	Adjusted *P* value	Difference (%) ± standard error	[Confidence intervals]	Adjusted *P* value
Inferior frontal gyrus	−32.2 ± 7.2	[−44.5, −17.2]	**0.046***	−25.2 ± 7.9	[−38.8, −8.6]	0.915
Orbitofrontal cortex	−20.3 ± 12.0	[−39.6, 5.3]	>1	−15.0 ± 12.8	[−35.7, 12.5]	>1
Frontal pole	−9.8 ± 16.3	[−35.2, 25.4]	>1	−25.5 ± 13.2	[−46.2, 3.1]	>1
Lingual gyrus	−37.1 ± 11.4	[−54.8, −12.4]	>1	−33.7 ± 11.8	[−52.2, −8.2]	>1
Precuneus	−24.1 ± 7.7	[−37.3, −7.9]	>1	−2.5 ± 9.8	[−19.4, 18.1]	>1
Occipital cortex	−23.9 ± 8.9	[−38.9, −5.2]	>1	−9.5 ± 10.5	[−27.3, 12.7]	>1
Precentral gyrus	−18.8 ± 7.5	[−31.9, −3.2]	>1	−8.6 ± 8.5	[−23.5, 9.1]	>1
Superior Temporal gyrus	−6.1 ± 8.9	[−21.7, 12.5]	>1	−23.0 ± 7.2	[−35.6, −7.9]	0.881
Middle frontal gyrus	−18.8 ± 7.8	[−32.5, −2.5]	>1	−15.4 ± 8.2	[−29.5, 1.6]	>1
Calcarine cortex	−39.7 ± 9.6	[−55.1, −19.0]	0.211	−25.6 ± 11.9	[−44.7, 0.1]	>1
Insula	−25.4 ± 10.8	[−43.0, −2.3]	>1	−24.0 ± 10.9	[−41.8, −0.8]	>1
Superior frontal gyrus	−8.4 ± 6.3	[−19.8, 4.7]	>1	−14.3 ± 5.9	[−25.0, −2.1]	>1
Supramarginal gyrus	−19.0 ± 8.7	[−33.9, −0.8]	>1	−15.5 ± 9.1	[−31.0, 3.5]	>1
Postcentral gyrus	−18.6 ± 7.7	[−32.0, −2.7]	>1	−11.4 ± 8.4	[−26.0, 6.0]	>1
Parahippocampal gyrus	−27.3 ± 17.3	[−52.5, 11.3]	>1	−40.0 ± 14.3	[−60.8, −8.2]	>1
Superior parietal lobule	−8.8 ± 7.8	[−22.6, 7.5]	>1	−10.4 ± 7.6	[−23.8, 5.5]	>1
Cuneus	−12.2 ± 13.9	[−34.4, 17.7]	>1	−7.7 ± 14.6	[−31.1, 23.7]	>1
Paracentral lobule	−5.8 ± 9.1	[−21.5, 13.2]	>1	−16.6 ± 8.1	[−30.6, 0.3]	>1
Inferior parietal lobule	−19.3 ± 7.4	[−32.2, −4.0]	>1	−14.8 ± 7.8	[−28.4, 1.5]	>1
Gyrus rectus	−39.2 ± 15.9	[−61.7, −3.6]	>1	−44.9 ± 14.6	[−65.5, −12.0]	>1
Latero-inferior temporal neocortex	−17.6 ± 7.8	[−31.2, −1.3]	>1	−19.9 ± 7.6	[−33.1, −4.2]	>1
Cingulate gyrus	−30.6 ± 9.6	[−46.3, −10.2]	>1	−34.5 ± 9.1	[−49.4, −15.2]	0.328

*Significant differences after correction for multiple comparisons.

Regional Growth of the Fetal Cortex and Transient Fetal Compartments

The fetal brain is composed of transient fetal compartments (Bystron et al. 2008). These fetal compartments are sights of major histogenic events that lead to their compartment-specific cyto- and myeloarchitecture (for review, see (Kostović et al. 2018b; Vasung et al. 2018, 2019)). The CP starts to appear around 9 GW and contains densely packed postmigratory neurons (Bystron et al. 2008). The SP, situated between the CP and intermediate zone (i.e., the fetal white matter), starts to appear a few weeks later, i.e., around 14 GW (Kostovic and Rakic 1990). However, in contrast to the CP, the SP contains rich extracellular matrix, dispersed postmigratory neurons, and, together with the marginal zone, the first axodendritic synapses (Molliver et al. 1973; Kostovic and Rakic 1990; Shatz 1992; Hanganu et al. 2001, 2009; Luhmann et al. 2009; Kanold and Luhmann 2010; Hoerder-Suabedissen and Molnár 2015; Kanold 2018; Kostović et al. 2018a). As expected, all regions of fetal cortex (composed of CP and SP) showed a significant positive association with age with a relative increase in volume ranging from 10 to 27% per GW.

During the mid-fetal and late-fetal periods (22–32 GW), the volume of the SP displays a growth spurt (Vasung et al. 2016). The growth spurt of the SP is characterized by a remarkable radial pattern of growth, that is, increase in SP thickness (Vasung et al. 2016). The radial growth of the SP has been explained by a "secondary expansion" concept (Duque et al. 2016). According to this concept, spatiotemporal accumulation of projection and association fibers, which "wait" within SP before their relocation to the CP, is most likely responsible for spatiotemporal differences observed in the SP thickness (Kostovic and Rakic 1990; Duque et al. 2016; Vasung et al. 2016; Kostović et al. 2018a). Around 32 GW, the volume of the SP reaches its peak occupying almost 45% of the telencephalic volume (Vasung et al. 2016). The period of development after 32GW is known as "SP resolution period," since after 32GW the SP undergoes reorganization and is difficult to identify continuously on MRI (Kostović et al. 2014; Vasung et al. 2016; Diogo et al. 2019).

Similar to the SP, during mid-fetal and late-fetal periods, the CP also grows exponentially (Vasung et al. 2016). However, its growth pattern is notably different from the growth pattern of the SP. Namely, the CP during these periods grows tangentially as the surface of the CP increases exponentially, while its thickness changes minimally (Vasung et al. 2016). The results in our study indicate that the relative volume of the SP compartment across all regions is similar to or smaller than the overlying CP. More specifically, no region had significantly higher relative volumes of SP compared to the CP after adjustment for age and sex. Given that SP thickness changes drastically during fetal development (Vasung et al. 2016), it is possible that tangential growth of the rigid CP, caused in part by ingrowth of axonal fibers and arborization of dendrites, leads to the appearance of cortical convolutions, which then exert biophysical forces on the underlying water-rich and jelly-like SP compartment. This hypothesis would partially explain the drastic age-dependent regional differences in the thickness of SP compartment (thinner below sulci) that parallel the synchronous increase of the relative volumes of CP and SP across the majority of cortical regions (observed in our study). However, these concepts remain to be tested using mathematical or deformable gel models (Tallinen et al. 2016; Foubet et al. 2018).

Table 4 Difference between females and males in the relative volume of the CP and SP

	CP			SP		
	Difference (%) ± standard error	[Confidence intervals]	Adjusted *P* value	Difference (%) ± standard error	[Confidence intervals]	Adjusted *P* value
Inferior frontal gyrus	−23.0 ± 7.8	[−36.5, −6.6]	>1	−34.1 ± 7.5	[−46.8, −18.3]	**0.045** *
Orbitofrontal cortex	−6.1 ± 13.3	[−27.9, 22.3]	>1	−27.8 ± 12.1	[−47.0, −1.6]	>1
Frontal pole	−8.1 ± 15.4	[−32.6, 25.2]	>1	−26.9 ± 14.5	[−49.0, 4.8]	>1
Lingual gyrus	−17.9 ± 13.6	[−39.5, 11.5]	>1	−49.2 ± 10.3	[−64.8, −26.7]	0.089
Precuneus	−7.8 ± 8.8	[−23.2, 10.6]	>1	−19.6 ± 8.9	[−34.8, −0.9]	>1
Occipital cortex	−7.5 ± 10.4	[−25.2, 14.4]	>1	−25.6 ± 9.2	[−41.0, −6.1]	>1
Precentral gyrus	−7.7 ± 8.3	[−22.1, 9.5]	>1	−19.6 ± 8.0	[−33.4, −3.0]	>1
Superior temporal gyrus	−10.1 ± 8.3	[−24.6, 7.1]	>1	−19.5 ± 8.0	[−33.4, −2.8]	>1
Middle frontal gyrus	−7.6 ± 8.6	[−22.5, 10.2]	>1	−25.7 ± 7.8	[−39.0, −9.5]	0.7
Calcarine cortex	−5.9 ± 13.7	[−28.2, 23.3]	>1	−52.3 ± 8.8	[−66.0, −33.1]	**0.009** *
Insula	−11.5 ± 12.1	[−31.4, 14.1]	>1	−35.9 ± 10.2	[−52.2, −14.0]	0.667
Superior frontal gyrus	−6.4 ± 6.1	[−17.5, 6.2]	>1	−16.1 ± 6.4	[−27.5, −3.0]	>1
Supramarginal gyrus	−12.4 ± 9.1	[−28.1, 6.7]	>1	−21.9 ± 8.9	[−37.0, −3.2]	>1
Postcentral gyrus	−12.1 ± 8.0	[−26.1, 4.5]	>1	−18.0 ± 8.3	[−32.4, −0.6]	>1
Parahippocampal gyrus	−12.4 ± 19.3	[−41.0, 30.2]	>1	−50.2 ± 13.5	[−69.2, −19.6]	0.8887
Superior parietal lobule	−5.7 ± 7.6	[−19.3, 10.1]	>1	−13.3 ± 8.2	[−27.5, 3.7]	>1
Cuneus	−7.7 ± 13.5	[−29.6, 21.0]	>1	−12.1 ± 15.8	[−36.8, 22.1]	>1
Paracentral lobule	−7.6 ± 8.4	[−22.2, 9.8]	>1	−14.9 ± 9.1	[−30.5, 4.2]	>1
Inferior parietal lobule	−7.3 ± 8.0	[−21.3, 9.3]	>1	−25.9 ± 7.5	[−38.9, −10.1]	0.531
Gyrus rectus	−24.8 ± 17.9	[−50.8, 15.1]	>1	−55.5 ± 13.6	[−73.9, −24.3]	0.624
Latero-inferior temporal neocortex	−15.8 ± 7.6	[−29.2, 0.1]	>1	−21.6 ± 8.0	[−35.4, −4.9]	>1
Cingulate gyrus	−12.4 ± 11.2	[−31.0, 11.3]	>1	−48.1 ± 8.2	[−61.2, −30.6]	**0.005** *

*Significant differences after correction for multiple comparisons

Furthermore, our results indicate that certain frontal, temporal, parietal, and limbic regions have significantly larger volumes of CP compared to the underlying SP. Thus, in these regions, it can be inferred that the average thickness of the SP compartment is most likely similar to or smaller than the CP. In contrast CP and SP in majority of parietal, precentral, and central regions had similar volumes. Our results are in agreement with the histological studies that showed very thin SP in limbic regions during prenatal development (Kostović and Krmpotić 1976) and thick SP in regions abundant with thalamocortical and corticocortical axons (Hanganu et al. 2009; Molnár and Hoerder-Suabedissen 2016; Kostović et al. 2018a).

In four regions, we found significant differences in relative growth rate between CP and SP. In superior temporal gyrus, the relative growth of the CP was significantly faster compared to the growth of the SP. In contrast, compared to the CP, the growth of SP was significantly faster in lingual gyrus, latero-inferior occipital cortex, and cuneus. The significant difference in the volumes and growth rate of CP and SP could indicate different amounts of thalamocortical and callosal fibers (Krsnik et al. 2017; Kostovic and Rakic 1990; LaMantia and Rakic 1990), some of which retract during the prenatal development (LaMantia and Rakic 1990). Furthermore, the inability to identify SP compartment continuously in all regions after 32 GW is in agreement with the seminal work of Kostovic and Rakic (1990) who suggested to refer to this stage of fetal brain development as the "subplate resolution stage." However, further work is needed to determine if these differences in growth result from predominantly radial or tangential expansion/retraction and which histogenic processes contribute to these differences.

Finally, in this work, we did not address if the differences in SP and CP growth between regions were statistically significant. Thus, we are unable to link spatiotemporal differences in histogenic processes and gene expression (described by e.g., (von Economo and Koskinas 1925; Kostovic and Rakic 1990; Jovanov-Milosević et al. 2009; Kang et al. 2011; Miller et al. 2014; Silbereis et al. 2016; Kostović et al. 2018a; Žunić Išasegi et al. 2018)) with the observations in our study. This is, however, within the scope of our future work.

Table 5 The difference in the relative volume of the cortex (CP and SP combined) between the left and right hemispheres

	Increase (%) ± standard error	[Confidence intervals]	Adjusted *P* value
Inferior frontal gyrus	25.6 ± 5.3	[15.7, 36.3]	**<0.001** *
Orbitofrontal cortex	−26.8 ± 5.6	[−36.7, −15.2]	**0.013** *
Frontal pole	33.7 ± 10.6	[14.8, 55.7]	0.0600
Lingual gyrus	33.4 ± 10.7	[14.3, 55.6]	0.0763
Precuneus	−12.3 ± 4.0	[−19.7, −4.2]	0.7404
Occipital cortex	−10.8 ± 3.6	[−17.6, −3.5]	0.9140
Precentral gyrus	−8.1 ± 3.1	[−14.0, −1.9]	>1
Superior temporal gyrus	−6.8 ± 2.8	[−12.1, −1.1]	>1
Middle frontal gyrus	−8.5 ± 3.6	[−15.2, −1.2]	>1
Calcarine cortex	−14.5 ± 6.4	[−26.0, −1.2]	>1
Insula	10.3 ± 7.1	[−2.7, 24.9]	>1
Superior frontal gyrus	−3.0 ± 2.7	[−8.2, 2.6]	>1
Supramarginal gyrus	3.7 ± 4.0	[−3.8, 11.7]	>1
Postcentral gyrus	−2.9 ± 3.7	[−9.9, 4.7]	>1
Parahippocampal gyrus	8.6 ± 13.1	[−13.4, 36.3]	>1
Superior parietal lobule	−2.5 ± 3.8	[−9.7, 5.3]	>1
Cuneus	−4.2 ± 8.2	[−18.7, 12.9]	>1
Paracentral lobule	−1.9 ± 4.8	[−10.8, 8.0]	>1
Inferior parietal lobule	1.8 ± 4.7	[−7.1, 11.4]	>1
Gyrus rectus	3.9 ± 15.6	[−21.3, 37.1]	>1
Latero-inferior temporal neocortex	−0.8 ± 3.8	[−7.9, 6.8]	>1
Cingulate gyrus	−0.6 ± 7.2	[−13.5, 14.1]	>1

*Significant differences after correction for multiple comparisons.

Regional Sex Differences in Relative Volumes of the Fetal Cortex and Transient Fetal Compartments

Differences in the brain structure and function between females and males have been studied from the beginning of neuroscience. For example, in addition to its larger absolute volumes, the brain of the adult male compared to the brain of the adult female displays more pronounced gray matter asymmetry in superior temporal regions (Guadalupe et al. 2015). The brain of the adult female has larger areas of gray matter, predominantly in frontal cortical regions (Ruigrok et al. 2014). Although sexually dimorphic patterns of brain development do exist and can be seen during childhood (Giedd et al. 1997), the regional volumetric differences are the most evident after puberty, that is, from 18 to 59 years of life (Ruigrok et al. 2014).

The prevalence of many neurodevelopmental disorders that have roots in prenatal brain development (Li et al. 2018), e.g., autism is different between males and females (Baron-Cohen et al. 2005). However, despite the growing knowledge about sexual dimorphism of the human postnatal brain, little is known about sexual dimorphism that occurs during prenatal brain development. It is generally accepted that the presence (or absence) of the sex-determining gene on the Y chromosome leads to the development of testicles (or ovaries) by 12 GW. In males, testosterone levels peak from 12 to 18 GW (Finegan et al. 1989) and again from 34 to 41GW (de Zegher et al. 1992). Thus, it is thought that these two windows of testosterone peaks fix the development of brain circuits through prenatal programming, which will be strongly influenced by high levels of testosterone during puberty. In our study, males compared to females had significantly larger relative volumes of the fetal cortex in left inferior frontal gyrus and significantly larger relative volumes of the "fiber waiting compartment" SP of inferior frontal gyrus, pericalcarine cortex, and cingulate gyrus (adjusted for hemisphere and age). In contrast, there was no significant difference between males and females in the regional growth rate of fetal cortex or transient fetal compartments. Thus, although our results indicate the absence of the sexual dimorphism in regional growth trajectories of the fetal cortex, they corroborate a hypothesis that requirements for establishing connectivity in specific regions of the fetal brain, such as inferior frontal gyrus, calcarine fissure, and cingulate gyrus, might be programmed differently between sexes. Whether sex differences in the volume of the SP reflect the rate of synaptogenesis (Alonso-Nanclares et al. 2008), cellular density (Amunts et al. 1999), or connectivity (Ingalhalikar et al. 2014) remains to be determined.

Regional Hemispheric Asymmetries in Relative Volumes of the Fetal Cortex and Transient Fetal Compartments

Hemispheric asymmetries of the cortical landscape have not been observed in postmortem pathology studies of fetuses during the early fetal development (Chi et al. 1977a, 1977b; Feess-Higgins and Larroche 1987). In agreement with autopsy studies, sophisticated MRI acquisition techniques using high-strength MRI on postmortem fetal brains during early fetal development (12–22 GW) have also reported the absence of structural asymmetries in the appearance of gyri and sulci as well as in the gross measurements such as volume and the length of the hemispheres (Zhang et al. 2013). However, after 22 GW, hemispheric asymmetries in folding patterns can be easily observed even with the in vivo MRIs. By 25 GW, both left and right superior temporal sulci are visible, with the right appearing around 23 GW followed by the left approximately at 25 GW (Kasprian et al. 2011; Habas et al. 2012). Measures of cortical curvature revealed that there are indeed hemispheric differences in the cortical curvature (Habas et al. 2012). In particular, the regions

Table 6 The difference in the relative volume of the CP and SP between the left and right hemisphere

	CP			SP		
	Difference (%) ± standard error	[Confidence intervals]	Adjusted *P* value	Difference (%) ± standard error	[Confidence intervals]	Adjusted *P* value
Inferior frontal gyrus	22.2 ± 6.5	[10.2, 35.4]	**0.0447***	29.0 ± 8.6	[13.5, 46.7]	**0.0337***
Orbitofrontal cortex	−24.1 ± 7.4	[−36.8, −8.7]	0.7276	−29.4 ± 8.6	[−43.8, −11.3]	0.6248
Frontal pole	7.2 ± 10.4	[−10.9, 29.0]	>1	66.7 ± 21.5	[31.0, 112.3]	**0.0142***
Lingual gyrus	32.5 ± 12.8	[10.3, 59.1]	0.5995	34.3 ± 17.5	[5.2, 71.4]	>1
Precuneus	−12.8 ± 4.9	[−21.8, −2.7]	>1	−11.9 ± 6.3	[−23.3, 1.1]	>1
Occipital cortex	−3.3 ± 4.8	[−12.3, 6.5]	>1	−17.8 ± 5.3	[−27.3, −6.9]	0.4562
Precentral gyrus	−6.1 ± 3.9	[−13.4, 1.7]	>1	−10.1 ± 4.8	[−18.9, −0.4]	>1
Superior temporal gyrus	−6.6 ± 3.5	[−13.2, 0.6]	>1	−7.0 ± 4.4	[−15.1, 1.9]	>1
Middle frontal gyrus	−10.3 ± 4.4	[−18.4, −1.4]	>1	−6.6 ± 5.7	[−17.0, 5.2]	>1
Calcarine cortex	−14.2 ± 7.6	[−27.6, 1.6]	>1	−14.7 ± 10.4	[−32.2, 7.3]	>1
Insula	4.5 ± 8.4	[−10.4, 21.9]	>1	16.3 ± 12.1	[−4.4, 41.6]	>1
Superior frontal gyrus	−1.4 ± 3.4	[−7.8, 5.5]	>1	−4.6 ± 4.3	[−12.5, 4.1]	>1
Supramarginal gyrus	1.5 ± 4.9	[−7.6, 11.5]	>1	5.9 ± 6.4	[−5.8, 19.0]	>1
Postcentral gyrus	−0.2 ± 4.8	[−9.1, 9.6]	0.9743	−5.5 ± 5.7	[−15.9, 6.2]	>1
Parahippocampal gyrus	4.3 ± 15.5	[−20.9, 37.5]	>1	13.1 ± 22.3	[−20.9, 61.8]	>1
Superior parietal lobule	−2.6 ± 4.7	[−11.4, 7.0]	>1	−2.3 ± 6.1	[−13.3, 10.1]	>1
Cuneus	−5.8 ± 10.1	[−23.0, 15.4]	>1	−2.6 ± 13.4	[−24.7, 25.9]	>1
Paracentral lobule	−1.0 ± 6.1	[−12.1, 11.5]	>1	−2.7 ± 7.5	[−16.2, 12.8]	>1
Inferior parietal lobule	6.0 ± 6.2	[−5.4, 18.7]	>1	−2.3 ± 7.2	[−15.2, 12.6]	>1
Gyrus rectus	24.4 ± 23.1	[−11.4, 74.7]	>1	−13.3 ± 21.2	[−43.9, 34.1]	>1
Latero-inferior temporal neocortex	−2.7 ± 4.6	[−11.2, 6.6]	>1	1.1 ± 6.1	[−10.0, 13.5]	>1
Cingulate gyrus	−10.0 ± 7.9	[−23.9, 6.4]	>1	9.7 ± 12.7	[−11.9, 36.5]	>1

*Significant differences after correction for multiple comparisons.

of superior temporal gyrus display significant hemispheric asymmetries since their posterosuperior parts tend to be more convex in the right hemisphere, while the regions belonging to the superior temporal sulcus tend to be more concave in the left hemisphere (Habas et al. 2012). However, despite the knowledge gained about hemispheric differences in the cortical curvature, little is known about hemispheric differences in the volume of transient fetal compartments in these regions. To our knowledge, there is only one study that showed hemispheric differences in the volume of the fetal tissue during prenatal development (Rajagopalan et al. 2011). According to the authors, from 20 to 28 GW, the superior temporal gyrus, in a small posterior region in proximity of transverse temporal gyri, displays regional rightward hemispheric asymmetry in volume (Rajagopalan et al. 2011). Later during development, after 31 GW, the left hemisphere not only shows a longer Sylvian fissure and a larger planum temporale but also has more frequently only one transverse temporal gyrus (Wada et al. 1975; Chi et al. 1977b). In contrast, the right hemisphere has more frequently two transverse temporal gyri and a shorter Sylvian fissure (Chi et al. 1977b).

Although we also observed hemispheric differences in the appearance of the superior temporal sulcus, we did not find hemispheric differences in the volumes of the superior temporal gyrus. It is possible that the smaller hemispheric differences in cortical and SP volume do exist but their effect size on the volume of the entire superior temporal gyrus is finer than the resolution of our imaging technique.

In contrast to the superior temporal gyrus, we did observe a significant leftward asymmetry in the relative volume of the CP and SP in the inferior frontal gyrus. This is in agreement with studies not only employing surface measurements (Falzi et al. 1982; Albanese et al. 1989) but also assessing the volume of the inferior frontal gyrus in adults. In a recently published asymmetry study in 17 141 healthy adult human brains, the authors reported leftward surface area asymmetry of the opercular part of the inferior frontal gyrus and a rightward surface area asymmetry of the triangular part of the inferior frontal gyrus (Kong et al. 2018). This is in agreement with the quantitative cytoarchitectonic studies demonstrating leftward asymmetry in the volume and cell packing density of the opercular part of the inferior frontal gyrus in the adult human brain (Amunts et al.

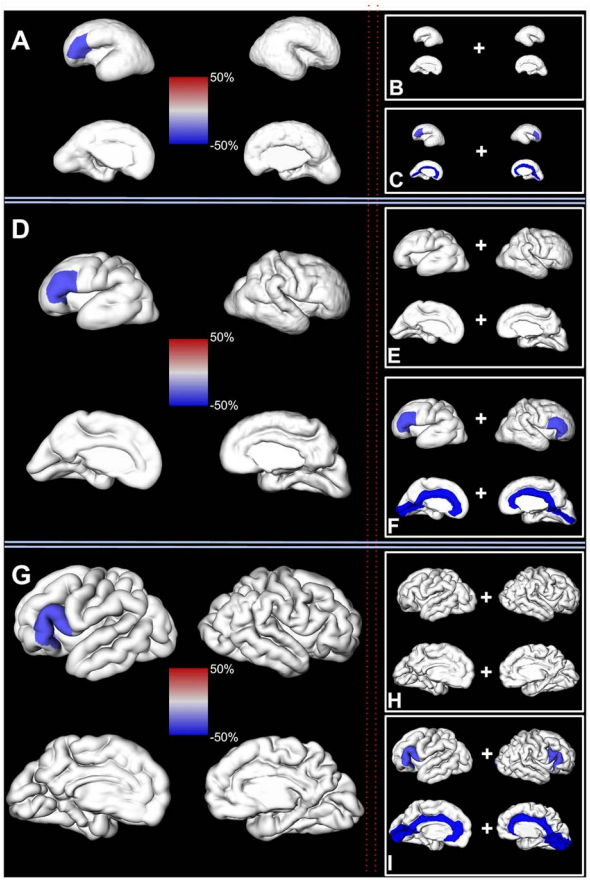

Figure 5. Significant regional sex differences in the human fetal brain. Left column: significant sex differences in the volume of the fetal cortex (composed of SP and CP) are shown on a reconstructed pial surface of 24.7 (*A*), 29.6 (*D*), and 35.29 (*G*) GW fetus. Positive regional sex differences (in red) indicate significantly larger volumes in females. Negative regional sex differences (in blue) indicate significantly larger volumes in males. The relative difference in the regional volumes between females and males (%) can be seen on the color-coded bars in the center. Note that the larger relative volumes of the inferior frontal gyrus for males. Right column: significant sex differences in the volume of the fetal compartments are shown on a reconstructed pial surface of the brains from the first column. (*B*, *E*, and *H*) Significant sex differences in the volume of the CP. (*C*, *F*, and *I*) Significant sex differences in the volume of the SP. Color coding of relative differences (%) is the same as in the left column.

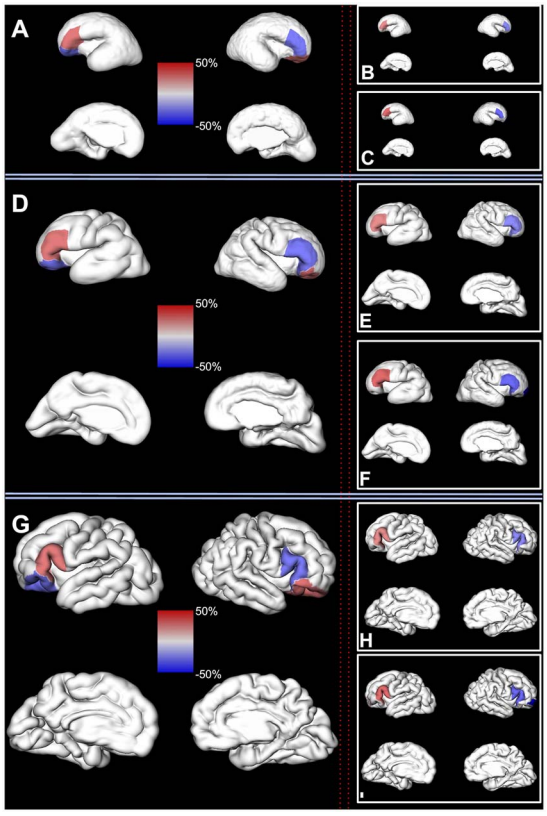

Figure 6. Hemispheric asymmetry. Left column: significant regional asymmetries in the volume of the fetal cortex (composed of SP and CP) are shown on a reconstructed pial surface of 24.7 (*A*), 29.6 (*D*), and 35.29 (*G*) GW fetus. Positive regional asymmetry indicates leftward asymmetry (in red). Negative regional asymmetry indicates rightward asymmetry (in blue). The relative difference (%) in the regional volume between left and right hemisphere can be seen on the color-coded bar in the center. Right column: significant regional asymmetries in the volume of the fetal compartments are shown on a reconstructed pial surface of the brain from the first column. (*B*, *E*, and *H*) Regional asymmetries in the volume of the CP. (*C*, *F*, and *I*) Regional asymmetries in the volume of the SP. Color coding of relative differences (%) is the same as in the left column.

1999). Given that the inferior frontal gyrus in our study included both opercular and triangular parts, it is possible that significant rightward hemispheric differences of this region become more evident after birth (Simonds and Scheibel 1989). To this end, significant leftward volumetric asymmetry of the SP belonging to the inferior frontal gyrus might play an important role in the early functional and structural reorganization of these language areas (Kostović and Judas 2007).

Finally, although we found significant rightward asymmetry in the relative volume of the orbitofrontal cortex, a separate analysis of the CP and SP of this region showed rightward asymmetry but did not yield significant results. Thus, it is possible that the discrete hemispheric differences of orbitofrontal cortex that exist in adults are also present in fetuses prenatally. However, the origins of these asymmetries should be explored with more detailed vertex and voxel approaches in the future.

Limitations

There were a few limitations in our study. Firstly, our parcellation of the fetal cortex was performed by one reader with extensive experience in segmenting the human fetal brain. Thus, in order to ensure unbiased parcellation of cortical regions, the reader was blind to the sex and hemisphere. Furthermore, manual delineation of the sulcal cerebrospinal fluid led to an underestimation of the cortical volume, in particular in older brains with numerous narrow sulci. In line with the aforementioned marginal zone, a thin transient fetal compartment situated between pia and the CP was most likely excluded from our analysis. Secondly, it is possible that there are smaller cortical subregions that display hemispheric asymmetries or sexual dimorphism. Those differences could be detected throughout the prenatal development by a voxel-based morphometry approach. However, in the third trimester, the morphology of the fetal brain changes tremendously, which limits reliable voxel-to-voxel registration. Finally, in several instances, sulci delimitation of specific regions (e.g., frontal pole, orbitofrontal cortex) was unreliable. Therefore, we relied on the visibility of fetal cortex in anterior, posterior, dorsal,

dorsolateral, medial, and ventral views. However, even with the reliable identification of the sulcal borders, projection of the labels from the surfaces to the volumes led to minor errors.

Conclusion

In conclusion, we identified cortical regions that show hemispheric asymmetries and sexual dimorphism in relative volumes of CP and SP during prenatal development. Significant leftward asymmetry was found in relative volumes of the CP and in relative volumes of SP in inferior frontal gyrus, while significant rightward asymmetry was found in the orbitofrontal cortex (CP and SP combined). Males showed significantly larger volumes of SP in inferior frontal gyrus, cingulate gyrus, and pericalcarine cortex. Given that observed hemispheric asymmetries and sexual dimorphism in relative volumes were not age-dependent, they could reflect cytoarchitectonic differences in the cellular composition of these regions that are genetically programmed during early fetal brain development.

Supplementary Material

Supplementary material is available at *Cerebral Cortex* online.

Funding

Ralph Schlaeger Foundation in Neuroradiology; National Institute of Neurological Disorders and Stroke of the National Institutes of Health (award number K23NS101120); American Academy of Neurology Clinical Research Training Fellowship; NARSAD Young Investigator Award from the Brain and Behavior Foundation; National Institutes of Health (grants R01EB018988, R01NS106030, and R01EB013248); Technological Innovations in Neuroscience Award from the McKnight Foundation.

Notes

We thank Claude Lepage for technical assistance with the MRI processing pipeline. The content is solely the responsibility of the authors and does not necessarily represent the official views of the National Institutes of Health, Ralph Schlaeger foundation, or the McKnight Foundation. *Conflict of Interest*: None declared.

References

Albanese E, Merlo A, Albanese A, Gomez E. 1989. Anterior speech region. Asymmetry and weight-surface correlation. *Arch Neurol*. 46:307–310.

Alonso-Nanclares L, Gonzalez-Soriano J, Rodriguez JR, DeFelipe J. 2008. Gender differences in human cortical synaptic density. *Proc Natl Acad Sci U S A*. 105:14615–14619.

Amunts K, Schleicher A, Bürgel U, Mohlberg H, Uylings HB, Zilles K. 1999. Broca's region revisited: cytoarchitecture and intersubject variability. *J Comp Neurol*. 412:319–341.

Avants BB, Tustison NJ, Song G, Cook PA, Klein A, Gee JC. 2011. A reproducible evaluation of ANTs similarity metric performance in brain image registration. *Neuroimage*. 54:2033–2044.

Bakken TE, Miller JA, Ding S-L, Sunkin SM, Smith KA, Ng L, Szafer A, Dalley RA, Royall JJ, Lemon T *et al*. 2016. A comprehensive transcriptional map of primate brain development. *Nature*. 535:367–375.

Baron-Cohen S, Knickmeyer RC, Belmonte MK. 2005. Sex differences in the brain: implications for explaining autism. *Science*. 310:819–823.

Brandler WM, Morris AP, Evans DM, Scerri TS, Kemp JP, Timpson NJ, St Pourcain B, Smith GD, Ring SM, Stein J *et al*. 2013. Common variants in left/right asymmetry genes and pathways are associated with relative hand skill. *PLoS Genet*. 9: e1003751.

Broca P. 1865. Sur le siège de la faculté du langage articulé (15 juin). *Bulletins de la Société Anthropologque de Paris*. 6: 377–393.

Büchel C, Raedler T, Sommer M, Sach M, Weiller C, Koch MA. 2004. White matter asymmetry in the human brain: a diffusion tensor MRI study. *Cereb Cortex*. 14:945–951.

Bystron I, Blakemore C, Rakic P. 2008. Development of the human cerebral cortex: Boulder committee revisited. *Nat Rev Neurosci*. 9:110–122.

Bystron I, Rakic P, Molnár Z, Blakemore C. 2006. The first neurons of the human cerebral cortex. *Nat Neurosci*. 9: 880–886.

Chi JG, Dooling EC, Gilles FH. 1977a. Gyral development of the human brain. *Ann Neurol*. 1:86–93.

Chi JG, Dooling EC, Gilles FH. 1977b. Left-right asymmetries of the temporal speech areas of the human fetus. *Arch Neurol*. 34:346–348.

Cunningham DJ. 1892. *Contribution to the Surface Anatomy of the Cerebral Hemispheres*. Dublin: Academy House.

Desikan RS, Ségonne F, Fischl B, Quinn BT, Dickerson BC, Blacker D, Buckner RL, Dale AM, Maguire RP, Hyman BT *et al*. 2006. An automated labeling system for subdividing the human cerebral cortex on MRI scans into gyral based regions of interest. *Neuroimage*. 31:968–980.

de Zegher F, Devlieger H, Veldhuis JD. 1992. Pulsatile and sexually dimorphic secretion of luteinizing hormone in the human infant on the day of birth. *Pediatr Res*. 32:605–607.

Diogo MC, Gruber GM, Bettelheim D, Kasprian G, Prayer D. 2018. OC06. 02: quantitative and qualitative evaluation of the visibility of brain lamination on T2-weighted and fluid-attenuated inversion recovery imaging. *Ultrasound Obstet Gynecol*. 52:12–12.

Diogo MC, Prayer D, Gruber GM, Brugger PC, Stuhr F, Weber M, Bettelheim D, Kasprian G. 2019. Echo-planar FLAIR sequence improves subplate visualization in fetal MRI of the brain. *Radiology*. 292:181976.

Dubois J, Benders M, Borradori-Tolsa C, Cachia A, Lazeyras F, Ha-Vinh Leuchter R, Sizonenko SV, Warfield SK, Mangin JF, Hüppi PS. 2008. Primary cortical folding in the human newborn: an early marker of later functional development. *Brain*. 131:2028–2041.

Duque A, Krsnik Z, Kostović I, Rakic P. 2016. Secondary expansion of the transient subplate zone in the developing cerebrum of human and nonhuman primates. *Proc Natl Acad Sci U S A*. 113:9892–9897.

Duvernoy HM. 2012. *The Human Brain: Surface, Three-Dimensional Sectional Anatomy with MRI, and Blood Supply*. Berlin: Springer Science & Business Media.

Eberstaller O. 1890. *Das Stirnhirn: ein Beitrag zur Anatomie der Oberfläche des Grosshirns*. Munich: Urban & Schwarzenberg.

Falzi G, Perrone P, Vignolo LA. 1982. Right-left asymmetry in anterior speech region. *Arch Neurol*. 39:239–240.

Feess-Higgins A, Larroche J-C. 1987. *Development of the Human Foetal Brain: An Anatomical Atlas*. Quebec: Institut National De LA Sante.

Finegan JA, Bartleman B, Wong PY. 1989. A window for the study of prenatal sex hormone influences on postnatal development. *J Genet Psychol*. 150:101–112.

Fogliarini C, Chaumoitre K, Chapon F, Fernandez C, Lévrier O, Figarella-Branger D, Girard N. 2005. Assessment of cortical maturation with prenatal MRI. Part I: normal cortical maturation. *Eur Radiol*. 15:1671–1685.

Foubet O, Trejo M, Toro R. 2018. Mechanical morphogenesis and the development of neocortical organisation. *Cortex*.

Frasnelli E. 2013. Brain and behavioral lateralization in invertebrates. *Front Psychol*. 4:939.

Garel C, Chantrel E, Brisse H, Elmaleh M, Luton D, Oury JF, Sebag G, Hassan M. 2001. Fetal cerebral cortex: normal gestational landmarks identified using prenatal MR imaging. *AJNR Am J Neuroradiol*. 22:184–189.

Germann J, Robbins S, Halsband U, Petrides M. 2005. Precentral sulcal complex of the human brain: morphology and statistical probability maps. *J Comp Neurol*. 493:334–356.

Geschwind N, Galaburda AM. 1985. Cerebral lateralization. Biological mechanisms, associations, and pathology: III. A hypothesis and a program for research. *Arch Neurol*. 42:634–654.

Gholipour A, Rollins CK, Velasco-Annis C, Ouaalam A, Akhondi-Asl A, Afacan O, Ortinau CM, Clancy S, Limperopoulos C, Yang E *et al*. 2017. A normative spatiotemporal MRI atlas of the fetal brain for automatic segmentation and analysis of early brain growth. *Sci Rep*. 7:476.

Giedd JN, Castellanos FX, Rajapakse JC, Vaituzis AC, Rapoport JL. 1997. Sexual dimorphism of the developing human brain. *Prog Neuropsychopharmacol Biol Psychiatry*. 21:1185–1201.

Girard N, Gambarelli D. 2001. *Normal Fetal Brain: Magnetic Resonance Imaging; An Atlas with Anatomic Correlations*. Brunelle F, Shaw D, Rickmansworth, UK, 2001..

Girard NJ, Dory-Lautrec P, Koob M, Dediu AM. 2012. MRI assessment of neonatal brain maturation. *Imaging Med*. 4:613–632.

Guadalupe T, Zwiers MP, Wittfeld K, Teumer A, Vasquez AA, Hoogman M, Hagoort P, Fernandez G, Buitelaar J, van Bokhoven H *et al*. 2015. Asymmetry within and around the human planum temporale is sexually dimorphic and influenced by genes involved in steroid hormone receptor activity. *Cortex*. 62:41–55.

Habas PA, Scott JA, Roosta A, Rajagopalan V, Kim K, Rousseau F, Barkovich AJ, Glenn OA, Studholme C. 2012. Early folding patterns and asymmetries of the normal human brain detected from in utero MRI. *Cereb Cortex*. 22:13–25.

Hanganu IL, Kilb W, Luhmann HJ. 2001. Spontaneous synaptic activity of subplate neurons in neonatal rat somatosensory cortex. *Cereb Cortex*. 11:400–410.

Hanganu IL, Okabe A, Lessmann V, Luhmann HJ. 2009. Cellular mechanisms of subplate-driven and cholinergic input-dependent network activity in the neonatal rat somatosensory cortex. *Cereb Cortex*. 19:89–105.

Hawrylycz MJ, Lein ES, Guillozet-Bongaarts AL, Shen EH, Ng L, Miller JA, van de Lagemaat LN, Smith KA, Ebbert A, Riley ZL *et al*. 2012. An anatomically comprehensive atlas of the adult human brain transcriptome. *Nature*. 489:391–399.

Heuer K, Gulban OF, Bazin PL, Osoianu A. 2018. Evolution of neocortical folding: a phylogenetic comparative analysis of MRI from 33 primate species. BioRxiv.

Hoerder-Suabedissen A, Molnár Z. 2015. Development, evolution and pathology of neocortical subplate neurons. *Nat Rev Neurosci*. 16:133–146.

Hrdlička A. 1907. *Measurements of the Cranial Fossae*. Washington: Smithsonian Institution, United States National Museum.

Huang H, Xue R, Zhang J, Ren T, Richards LJ, Yarowsky P, Miller MI, Mori S. 2009. Anatomical characterization of human fetal brain development with diffusion tensor magnetic resonance imaging. *J Neurosci*. 29:4263–4273.

Iaria G, Petrides M. 2007. Occipital sulci of the human brain: variability and probability maps. *J Comp Neurol*. 501:243–259.

Ingalhalikar M, Smith A, Parker D, Satterthwaite TD, Elliott MA, Ruparel K, Hakonarson H, Gur RE, Gur RC, Verma R. 2014. Sex differences in the structural connectome of the human brain. *Proc Natl Acad Sci U S A*. 111:823–828.

Jovanov-Milosević N, Culjat M, Kostović I. 2009. Growth of the human corpus callosum: modular and laminar morphogenetic zones. *Front Neuroanat*. 3:6.

Judaš M, Radoš M, Jovanov-Milošević N, Hrabac P, štern-Padovan R, Kostović I. 2005. Structural, immunocytochemical, and MR imaging properties of periventricular crossroads of growing cortical pathways in preterm infants. *AJNR Am J Neuroradiol*. 26:2671–2684.

Kainz B, Steinberger M, Wein W, Kuklisova-Murgasova M, Malamateniou C, Keraudren K, Torsney-Weir T, Rutherford M, Aljabar P, Hajnal JV *et al*. 2015. Fast volume reconstruction from motion corrupted stacks of 2D slices. *IEEE Trans Med Imaging*. 34:1901–1913.

Kang HJ, Kawasawa YI, Cheng F, Zhu Y, Xu X, Li M, Sousa AMM, Pletikos M, Meyer KA, Sedmak G *et al*. 2011. Spatio-temporal transcriptome of the human brain. *Nature*. 478:483–489.

Kanold PO. 2018. The first cortical circuits: subplate neurons lead the way and shape cortical organization. *Neuroforum*. 25:15–23.

Kanold PO, Luhmann HJ. 2010. The subplate and early cortical circuits. *Annu Rev Neurosci*. 33:23–48.

Karolis VR, Corbetta M, Thiebaut de Schotten M. 2019. The architecture of functional lateralisation and its relationship to callosal connectivity in the human brain. *Nat Commun*. 10:1417.

Kasprian G, Langs G, Brugger PC, Bittner M, Weber M, Arantes M, Prayer D. 2011. The prenatal origin of hemispheric asymmetry: an in utero neuroimaging study. *Cereb Cortex*. 21:1076–1083.

Kidokoro H, Anderson PJ, Doyle LW, Neil JJ, Inder TE. 2011. High signal intensity on T2-weighted MR imaging at term-equivalent age in preterm infants does not predict 2-year neurodevelopmental outcomes. *AJNR Am J Neuroradiol*. 32:2005–2010.

Kong X-Z, Mathias SR, Guadalupe T, ENIGMA Laterality Working Group, Glahn DC, Franke B, Crivello F, Tzourio-Mazoyer N, Fisher SE, Thompson PM *et al*. 2018. Mapping cortical brain asymmetry in 17,141 healthy individuals worldwide via the ENIGMA consortium. *Proc Natl Acad Sci U S A*. 115:E5154–E5163.

Kostović I, Išasegi IŽ, Krsnik Ž. 2018a. Sublaminar organization of the human subplate: developmental changes in the distribution of neurons, glia, growing axons and extracellular matrix. *J Anat*. .

Kostović I, Jovanov-Milošević N, Radoš M, Sedmak G, Benjak V, Kostović-Srzentić M, Vasung L, Čuljat M, Radoš M, Hüppi P *et al*. 2014. Perinatal and early postnatal reorganization of the subplate and related cellular compartments in the human cerebral wall as revealed by histological and MRI approaches. *Brain Struct Funct*. 219:231–253.

Kostović I, Judas M. 2007. Transient patterns of cortical lamination during prenatal life: do they have implications for treatment? *Neurosci Biobehav Rev*. 31:1157–1168.

Kostović I, Judas M, Rados M, Hrabac P. 2002. Laminar organization of the human fetal cerebrum revealed by histochemical markers and magnetic resonance imaging. *Cereb Cortex*. 12:536–544.

Kostović I, Krmpotić J. 1976. Early prenatal ontogenesis of the neuronal connections in the interhemispheric cortex of the human gyrus cinguli. *Verh Anat Ges*. 305–316.

Kostovic I, Rakic P. 1990. Developmental history of the transient subplate zone in the visual and somatosensory cortex of the macaque monkey and human brain. *J Comp Neurol*. 297:441–470.

Kostović I, Sedmak G, Judaš M. 2018b. Neural histology and neurogenesis of the human fetal and infant brain. *Neuroimage*. 188:743–773.

Krsnik Ž, Majić V, Vasung L, Huang H, Kostović I. 2017. Growth of thalamocortical fibers to the somatosensory cortex in the human fetal brain. *Front Neurosci*. 11:1780.

LaMantia AS, Rakic P. 1990. Axon overproduction and elimination in the corpus callosum of the developing rhesus monkey. *J Neurosci*. 10:2156–2175.

Leach EL, Prefontaine G, Hurd PL, Crespi BJ. 2014. The imprinted gene LRRTM1 mediates schizotypy and handedness in a nonclinical population. *J Hum Genet*. 59:332–336.

Leuret F, Gratiolet P. 1839. *Anatomie comparée du système nerveux, considérée dans ses rapports avec l'intelligence*. Vol 1-2. Paris: Baillière.

Li M, Santpere G, Kawasawa YI, Evgrafov OV, Gulden FO, Pochareddy S, Sunkin SM, Li Z, Shin Y, Zhu Y *et al*. 2018. Integrative functional genomic analysis of human brain development and neuropsychiatric risks. *Science*. 362: eaat7615.

Luhmann HJ, Kilb W, Hanganu-Opatz IL. 2009. Subplate cells: amplifiers of neuronal activity in the developing cerebral cortex. *Front Neuroanat*. 3:19.

Matsuo R, Kawaguchi E, Yamagishi M, Amano T, Ito E. 2010. Unilateral memory storage in the procerebrum of the terrestrial slug Limax. *Neurobiol Learn Mem*. 93:337–342.

Medland SE, Duffy DL, Wright MJ, Geffen GM, Hay DA, Levy F, van-Beijsterveldt CEM, Willemsen G, Townsend GC, White V *et al*. 2009. Genetic influences on handedness: data from 25,732 Australian and Dutch twin families. *Neuropsychologia*. 47:330–337.

Miller JA, Ding S-L, Sunkin SM, Smith KA, Ng L, Szafer A, Ebbert A, Riley ZL, Royall JJ, Aiona K *et al*. 2014. Transcriptional landscape of the prenatal human brain. *Nature*. 508: 199–206.

Mohseni Salehi SS, Erdogmus D, Gholipour A. 2017. Auto-context convolutional neural network (auto-net) for brain extraction in magnetic resonance imaging. *IEEE Trans Med Imaging*. 36:2319–2330.

Molliver ME, Kostović I, van der Loos H. 1973. The development of synapses in cerebral cortex of the human fetus. *Brain Res*. 50:403–407.

Molnár Z, Hoerder-Suabedissen A. 2016. Regional scattering of primate subplate. *Proc Natl Acad Sci U S A*. 113:9676–9678.

Ocklenburg S, Arning L, Gerding WM, Epplen JT, Güntürkün O, Beste C. 2013. FOXP2 variation modulates functional hemispheric asymmetries for speech perception. *Brain Lang*. 126:279–284.

Ono M, Kubik S, Abernathey CD, Yaşargil MG. 1990. *Atlas of the Cerebral Sulci*. Stuttgart: Georg Thieme Verlag.

Perkins L, Hughes E, Srinivasan L, Allsop J, Glover A, Kumar S, Fisk N, Rutherford M. 2008. Exploring cortical subplate evolution using magnetic resonance imaging of the fetal brain. *Dev Neurosci*. 30:211–220.

Pletikos M, Sousa AMM, Sedmak G, Meyer KA, Zhu Y, Cheng F, Li M, Kawasawa YI, Sestan N. 2014. Temporal specification and bilaterality of human neocortical topographic gene expression. *Neuron*. 81:321–332.

Rajagopalan V, Scott J, Habas PA, Kim K, Corbett-Detig J, Rousseau F, Barkovich AJ, Glenn OA, Studholme C. 2011. Local tissue growth patterns underlying normal fetal human brain gyrification quantified in utero. *J Neurosci*. 31:2878–2887.

Retzius G. 1896. *Das Menschenhirn: Studien in der Makroskopischen Morphologie*. Stochkolm: P.A.Norsted.

Robinson KJ, Hurd PL, Read S, Crespi BJ. 2016. The PCSK6 gene is associated with handedness, the autism spectrum, and magical ideation in a non-clinical population. *Neuropsychologia*. 84:205–212.

Rogers LJ, Anson JM. 1979. Lateralisation of function in the chicken fore-brain. *Pharmacol Biochem Behav*. 10:679–686.

Ruigrok ANV, Salimi-Khorshidi G, Lai M-C, Baron-Cohen S, Lombardo MV, Tait RJ, Suckling J. 2014. A meta-analysis of sex differences in human brain structure. *Neurosci Biobehav Rev*. 39:34–50.

Scerri TS, Brandler WM, Paracchini S, Morris AP, Ring SM, Richardson AJ, Talcott JB, Stein J, Monaco AP. 2011. PCSK6 is associated with handedness in individuals with dyslexia. *Hum Mol Genet*. 20:608–614.

Segal E, Petrides M. 2012. The morphology and variability of the caudal rami of the superior temporal sulcus. *Eur J Neurosci*. 36:2035–2053.

Shatz CJ. 1992. How are specific connections formed between thalamus and cortex? *Curr Opin Neurobiol*. 2:78–82.

Silbereis JC, Pochareddy S, Zhu Y, Li M, Sestan N. 2016. The cellular and molecular landscapes of the developing human central nervous system. *Neuron*. 89:248–268.

Simonds RJ, Scheibel AB. 1989. The postnatal development of the motor speech area: a preliminary study. *Brain Lang*. 37:42–58.

Smaers JB. 2013. How humans stand out in frontal lobe scaling. *Proc Natl Acad Sci U S A*. 110:E3682.

Smith GE. 1904a. *Studies in the Morphology of the Human Brain: With Special Reference to that of the Egyptians. The Occipital Region*. Cairo: National Printing Department.

Smith GE. 1904b. The morphology of the retrocalcarine region of the cortex cerebri. *Proc R Soc Lond*. 73:59–65.

Tallinen T, Chung JY, Rousseau F, Girard N, Lefèvre J, Mahadevan L. 2016. On the growth and form of cortical convolutions. *Nat Phys*. 12:588.

Tustison NJ, Avants BB, Cook PA, Zheng Y, Egan A, Yushkevich PA, Gee JC. 2010. N4ITK: improved N3 bias correction. *IEEE Trans Med Imaging*. 29:1310–1320.

Vasung L, Abaci Turk E, Ferradal SL, Sutin J, Stout JN, Ahtam B, Lin P-Y, Grant PE. 2018. Exploring early human brain development with structural and physiological neuroimaging. *Neuroimage*. .

Vasung L, Charvet CJ, Shiohama T, Gagoski B, Levman J, Takahashi E. 2019. Ex vivo fetal brain MRI: recent advances, challenges, and future directions. *Neuroimage*. .

Vasung L, Huang H, Jovanov-Milošević N, Pletikos M, Mori S, Kostović I. 2010. Development of axonal pathways in the human

fetal fronto-limbic brain: histochemical characterization and diffusion tensor imaging. *J Anat*. 217:400–417.

Vasung L, Lepage C, Radoš M, Pletikos M, Goldman JS, Richiardi J, Raguž M, Fischi-Gómez E, Karama S, Huppi PS *et al*. 2016. Quantitative and qualitative analysis of transient fetal compartments during prenatal human brain development. *Front Neuroanat*. 10:11.

Vasung L, Raguz M, Kostovic I, Takahashi E. 2017. Spatiotemporal relationship of brain pathways during human fetal development using high-angular resolution diffusion MR imaging and histology. *Front Neurosci*. 11:348.

von Economo CF, Koskinas GN. 1925. Die cytoarchitektonik der hirnrinde des erwachsenen menschen. *J. Springer*.

Wada JA, Clarke R, Hamm A. 1975. Cerebral hemispheric asymmetry in humans: cortical speech zones in 100 adult and 100 infant brains. *Arch Neurol*. 32:239–246.

Yun HJ, Chung AW, Vasung L, Yang E, Tarui T, Rollins CK, Ortinau CM, Grant PE, Im K. 2018. Automatic labeling of cortical sulci for the human fetal brain based on spatio-temporal information of gyrification. *Neuroimage*.

Zhang Z, Hou Z, Lin X, Teng G, Meng H, Zang F, Fang F, Liu S. 2013. Development of the fetal cerebral cortex in the second trimester: assessment with 7T postmortem MR imaging. *AJNR Am J Neuroradiol*. 34: 1462–1467.

Zlatkina V, Petrides M. 2010. Morphological patterns of the postcentral sulcus in the human brain. *J Comp Neurol*. 518:3701–3724.

Žunić Išasegi I, Radoš M, Krsnik Ž, Radoš M, Benjak V, Kostović I. 2018. Interactive histogenesis of axonal strata and proliferative zones in the human fetal cerebral wall. *Brain Struct Funct*. 223:3919–3943.